Steady state of a fully detuned storage-ring free-electron laser

G. De Ninno,[1,2,*] C. Bruni,[1] D. Nutarelli,[3] D. Garzella,[1,2] C. Thomas,[1,4] and M. E. Couprie[1,2]
[1]*CEA/DSM/DRECAM, Gif-sur-Yvette, France*
[2]*LURE, Orsay, France*
[3]*LAC, Orsay, France*
[4]*Eindhoven University, Eindhoven, The Netherlands*
(Received 5 September 2002; published 13 February 2003)

This paper gives an analytical description of the stationary regime of a storage-ring free-electron laser in the presence of the maximum detuning (compatible with the laser onset) between the laser pulse and the electron beam when they pass and interact in the optical cavity. In this condition, the conservation of the first moments of the laser intensity distribution allows one to express the peak gain of the light amplification process and the maximum detuning as a function of system parameters that are directly measurable. These theoretical results are compared with experiments performed on the Super-ACO free-electron laser.

DOI: 10.1103/PhysRevE.67.026501 PACS number(s): 41.60.Cr, 29.20.Dh

I. INTRODUCTION

Storage-ring free-electron lasers (SRFELs) are complex, strongly coupled dynamical systems, which are based on the interaction between a highly relativistic electron beam circulating in a storage ring and an electromagnetic wave stored in an optical cavity. The laser effect originates from the radiation emitted by the electrons when they pass through the magnetic field generated by an insertion device (e.g., an undulator). Once stored in the optical cavity, the radiation is amplified by successive interactions with the electron beam. This process generally leads to the increase of the electron-beam energy spread and, as a consequence, to the reduction of the amplification gain, until this latter reaches the level of the cavity losses. Since it originates from the synchrotron radiation, the laser is naturally pulsed at the electron-beam revolution period (hundreds of nanoseconds). On a larger (millisecond) temporal scale, the FEL dynamics depends strongly on the longitudinal overlap between the electron bunch(es) and the laser pulses at each pass inside the optical cavity. A given temporal detuning, i.e., a difference between the electron-beam revolution period and the photon round trip inside the optical cavity, leads to a cumulative delay between the electrons and the laser pulses: the laser intensity may then appear to be ''cw'' (for a weak or strong detuning) or show a stable pulsed behavior (for an intermediate detuning amount) [1–3]. Figure 1 presents the FEL intracavity power as a function of the laser–electron-beam detuning, as it is measured in the case of the Super-ACO FEL. Together with the laser induced energy spread, which results in a reduction of the electron density, the laser-electron beam detuning is the main process leading a SRFEL to saturation [4]. In fact, a detuned laser grows interacting with a reduced electron density and therefore having at disposal a smaller peak gain with respect to the zero-detuning case.

The dynamics of a SRFEL can be generally described by a system of integro-differential coupled equations accounting for the evolution of the electromagnetic field and the longitudinal parameters of the electron bunch [5–7,4,8–11]. The strong laser–electron-beam coupling originates from the fact that, unlike a LINAC based FEL, where the beam is renewed after each interaction, electrons are recirculated. As a consequence, at every light–electron-beam energy exchange, the system keeps memory of previous interactions.

The optical pulse propagation in FELs has been discussed in a number of papers. Due to its high mathematical complexity, the problem has been generally treated using a numerical approach (see Ref. [12] for a general review of the obtained results). The most significant analytical results have been obtained in Refs. [6,7], yielding a deep insight into the physics of the process. In practice, the laser electric field, assumed to be centered around the maximum of the temporal electron-bunch distribution (i.e., quasizero laser–electron-

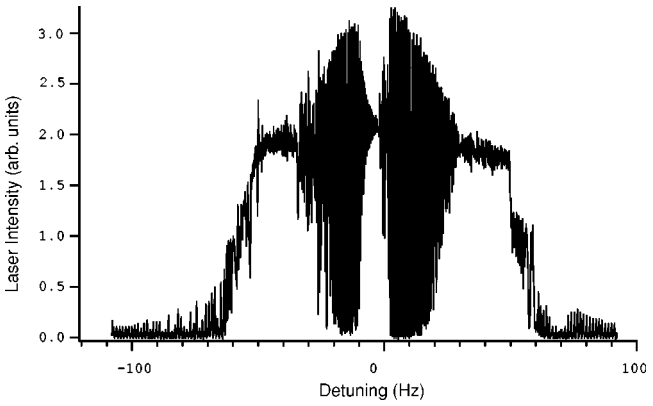

FIG. 1. Laser intensity of the Super-ACO FEL as a function of the laser–electron-beam detuning. The detuning is expressed in terms of the variation Δf_{RF} of the main cavity frequency with respect to the perfect tuning (the variation of 1 Hz corresponding to a laser–electron-beam delay of 1.2 fs). In order to span Δf_{RF} continuously, a sweeping ramp has been applied to the radio-frequency plot. The parameters characterizing the employed experimental setting are the following: Electron-beam energy = 800 MeV, interpulse period (two-bunch operation) = 120 ns, beam current $\simeq$40 mA, laser wavelength = 350 nm, small signal gain $g_0 \simeq 1.4\%$, cavity losses $P \simeq 0.5\%$. The accelerator has been operated with the harmonic cavity set in the passive configuration.

*Present address: Sincrotrone Trieste, 34012 Trieste, Italy.

 ©2003 The American Physical Society

beam detuning), is decomposed on a basis of longitudinal modes (the so-called supermodes) self-reproducing in form after each round trip. After many round trips, the system evolves towards the fundamental supermode, which is characterized by a Gaussian profile. In most cases, this result has been found to be in a good agreement with experiments [13,14], and it will be taken as one of the starting points of the analysis that will be developed in the following.

It is worthwhile to stress that, while a considerable effort (both theoretical and experimental) has been made in the past in order to characterize the laser pulse propagation close to perfect tuning, an exhaustive analysis of the detuned SRFEL dynamics is still lacking. On the other hand, the investigation of the detuned regime of a SRFEL proves to be essential in order to acquire a complete mastery of the laser source. In fact, as it is shown in Fig. 1, the behavior of the system at the perfect tuning can be maintained only in a narrow range of the detuning parameter (normally by means of a feedback system [15,16]). Such a behavior is just a particular case of a much more complex dynamics, the knowledge of which has to be considered as a fundamental tool for a proper run of users' experiments.

This paper intends to give an analytical description of the FEL stationary regime in the presence of maximum detuning compatible with the laser onset. When the system is in this fully detuned condition, the equation governing its evolution can be considerably simplified. In fact, the conservation of the first moments of the laser temporal distribution, once the steady state is reached, allows one to derive a simple analytical formula for the laser-off peak gain g_0 (alternative to that derived from Madey's theorem [17]) as well as a relation giving the full width of the detuning curve. These theoretical results will be compared with experiments for the case of the Super-ACO FEL.

II. THE FEL GAIN

The gain of a SRFEL depends on both the electron-beam parameters and the insertion device characteristics. It can be generally written as the derivative of the radiation emitted by the electrons in the insertion device (the so-called ''spontaneous emission'') with respect to the electron-beam energy [18,17]. The insertion device that is usually employed in a SRFEL is an optical klystron [19], which is composed of two undulators separated by a dispersive section (i.e., a strong magnetic field) favoring the interference between the emission of the undulators. This results in an enhanced amplification gain with respect to the single-undulator configuration.

When the laser pulse is well established, it has an extremely narrow spectral profile centered around the resonant wavelength

$$\lambda_r = \frac{\lambda_0}{2\gamma^2}\left(1+\frac{K^2}{2}\right), \tag{1}$$

where λ_0 is the undulator period, γ is the Lorentz factor, and $K=(eB_0\lambda_0)/(2\pi mc)$ is the undulator deflection parameter (B_0 being the maximum magnetic field along the undulator axis, λ_0 the magnetic period, e and m the electron mass and charge, c the light speed). Under this assumption, the gain can be expressed in the form[1] [17]

$$g(\tau) = g_0 \frac{f}{f_0}\frac{\rho_e(\tau)}{\hat{\rho}_{e0}}, \tag{2}$$

where τ stands for the temporal position with respect to the centroid of the electron-bunch distribution, g_0 is the small-signal gain, i.e., the maximum gain when the laser is off, f is the modulation rate of the optical klystron spectrum (depending on the rms value of the temporal beam distribution), f_0 its laser-off value, $\rho_e(\tau)$ is the electron density, and $\hat{\rho}_{e0}$ its laser-off peak value.

According to Madey's theorem [18], the laser-off peak gain is given by

$$g_0 = 2.2\times 10^{-13}(KL)^2(JJ)^2(N+N_d)\frac{f_0\hat{\rho}_{e0}F_f}{\gamma^3}, \tag{3}$$

where L is the length of one undulator, $JJ=J_0(\xi)-J_1(\xi)$ is the difference between the Bessel function of zero and first order [$\xi=K^2/(4+2K^2)$], N is the number of undulator periods, N_d is the interference order, and F_f is the so-called filling factor [20], taking into account the transverse overlap between the electrons and photons.

Equation (2) shows that the optical gain as a function of the beam current can be determined by measuring the statistical parameters of the electron beam: the transverse dimensions and the bunch length, which give the electron density, and the beam energy spread, which is related to the modulation rate.

A more direct estimation of the optical gain can be performed by measuring the initial growth rate of the laser intensity, which is inversely proportional to the difference between the peak gain and the optical cavity losses. The knowledge of the cavity losses also allows one to determine the gain corresponding to the beam current threshold for the laser oscillation.

III. DYNAMICS OF A FULLY DETUNED SRFEL

The rate equation for the evolution of the laser intensity I can be written in the form [11]

$$I_{n+1}(\tau) = R^2[1+g_n(\tau-\delta\tau)]I_n(\tau-\delta\tau)+I_s(\tau-\delta\tau), \tag{4}$$

where n is the iteration number (labeling the number of laser–electron-beam interactions inside the optical klystron), $R^2=1-P$ stands for the total reflectivity of the cavity mirrors (P being the total cavity losses), I_s is the spontaneous emission of the optical klystron, and $\delta\tau=T_b-T_l$ (where T_b

[1]Here and in the following, the slippage effect due to the different velocity of electrons with respect to photons during a single passage inside the interaction region is neglected. This assumption is generally allowed as far as SRFELs are concerned.

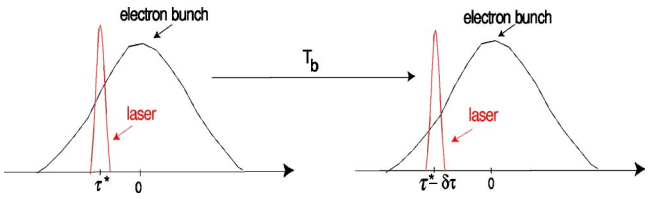

FIG. 2. (Color online) Schematic layout of the pass-to-pass laser–electron-beam interaction. T_b stands for the period between two successive electron bunches, τ^* is the position of the laser centroid with respect to the peak of the electron density, and $\delta\tau$ (here assumed to be positive) accounts for the laser–electron-beam detuning at each pass.

is the time interval between two successive electron bunches and T_l is the oscillation period of the laser pulse inside the optical cavity) accounts for the temporal detuning between the electron bunch and the laser pulse at each pass inside the optical cavity (see Fig. 2).

Since the proper laser mode of the optical cavity is already established after a few hundred light paths, the longitudinal and transverse laser dynamics are assumed to be decoupled and the latter is disregarded here. Assuming that the electron-bunch temporal distribution keeps its "natural" Gaussian profile under the action of the laser growth, the gain of the amplification process when the laser is fully detuned (i.e., $\delta\tau=\delta\tau_m$, where m stands for maximum) becomes

$$g(\tau)=g_0\exp\left(-\frac{\tau^2}{2\sigma_e^2}\right), \tag{5}$$

where, with respect to Eq. (2), it has been also assumed that the laser onset does not affect the electron-beam distribution (i.e., $f=f_0$ and $\hat{\rho}_e=\hat{\rho}_{e0}$, where $\hat{\rho}_e$ is the peak value of the electron density). In other words, one can suppose that the saturation process of a fully detuned FEL does not depend on the laser induced energy spread but is only driven by the laser–electron-beam temporal delay.

It is worthwhile to stress that the Gaussian hypothesis on the bunch temporal profile also entails that the interaction of the electron beam with the ring environment [21–23] is neglected. This important point will be further discussed in the following section.

Combining Eqs. (5) and (4), one gets ($I_s \ll I_n$)

$$I_{n+1}(\tau)=R^2\left\{1+g_0\exp\left[-\frac{(\tau-\delta\tau_m)^2}{2\sigma_e^2}\right]\right\}I_n(\tau-\delta\tau_m). \tag{6}$$

Assume now that the laser reaches a stationary regime [$I_{n+1}(\tau)=I_f(\tau)$, where f stands for final] and suppose that the stationary laser distribution is characterized by a Gaussian shape, i.e.,

$$I_n(\tau)\equiv I(\tau)=I_0\exp[-(\tau-\tau_0)^2/2\sigma_l^2] \tag{7}$$

(where τ_0 is the position of the laser centroid when the detuning is maximum, σ_l is the rms width of the laser distribution, and I_0 is the peak laser intensity). The Gaussian hypothesis can be considered as a tentative extension of the result obtained in the framework of the supermodes theory [6,7] for a perfect laser–electron-beam overlapping to the case of a fully detuned FEL.

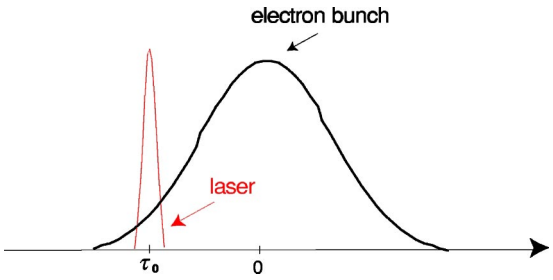

FIG. 3. (Color online) Schematic layout of the laser stationary regime when the light pulse and the electron bunch are fully detuned (a positive detuning is assumed).

Under the conditions specified above, the equation for the equilibrium regime becomes [24,25]

$$I_f(\tau)=R^2I_0\exp[-(\tau-\tau_0-\delta\tau_m)^2/2\sigma_l^2]\times\left\{1+g_0\exp\left[-\frac{(\tau-\delta\tau_m)^2}{2\sigma_e^2}\right]\right\}. \tag{8}$$

By definition, when the laser reaches the stationary regime, the first moments of its distribution stay constant under the effect of subsequent laser–electron-beam interactions.

A. Conservation of the zero-order moment

The conservation of the zero-order moment of the laser distribution

$$\int_{-\infty}^{+\infty}I_f(\tau)d\tau=\int_{-\infty}^{+\infty}I(\tau)d\tau \tag{9}$$

is equivalent to that of the laser intensity. Making use of Eq. (8) and solving the integrals, this condition leads to the following relation:

$$R^2\left\{1+\frac{g_0\exp\{-\tau_0^2/[2(\sigma_e^2+\sigma_l^2)]\}}{\sqrt{1+(\sigma_l/\sigma_e)^2}}\right\}=1, \tag{10}$$

that is ($P=1-R^2$),

$$g_0=\frac{P}{1-P}\sqrt{1+(\sigma_l/\sigma_e)^2}\exp\{\tau_0^2/[2(\sigma_e^2+\sigma_l^2)]\}. \tag{11}$$

The details of the calculation are reported in the Appendix.

This formula expresses the laser-off peak gain as a function of the cavity losses and of the statistical parameters of the laser and electron-beam distributions. Assuming $P\ll 1$ and $\sigma_l\ll\sigma_e$, it reduces to $g_0\exp(-\tau_0^2/2\sigma_e^2)=P$, which is the usual equilibrium condition neglecting the width of the laser profile. Figure 3 shows a schematic layout of the stationary regime of the laser distribution when the light pulse and the electron bunch are fully detuned.

B. Conservation of the first-order moment

The condition

$$\int_{-\infty}^{+\infty} \tau I_f(\tau)\, d\tau = \int_{-\infty}^{+\infty} \tau I(\tau)\, d\tau \tag{12}$$

is equivalent to the conservation of the temporal position of the laser centroid: $\tau_f = \tau_0$ (where τ_f is the centroid position of the distribution I_f). Making use of Eqs. (8) and (11), one gets (see the Appendix for the details of the calculation)

$$\begin{aligned}\tau_f &\equiv \frac{\int_{-\infty}^{+\infty} \tau I_f(\tau)\, d\tau}{\int_{-\infty}^{+\infty} I_f(\tau)\, d\tau} \\ &= \tau_0 \left[\frac{1 + \dfrac{g_0 \exp\{-\tau_0^2/[2(\sigma_e+\sigma_l)^2]\}}{[1+(\sigma_l/\sigma_e)^2]\sqrt{1+(\sigma_l/\sigma_e)^2}}}{1 + \dfrac{g_0 \exp\{-\tau_0^2/[2(\sigma_e+\sigma_l)^2]\}}{\sqrt{1+(\sigma_l/\sigma_e)^2}}} \right] + \delta\tau_m \\ &= \tau_0 \frac{1+R^2(\sigma_l/\sigma_e)^2}{1+(\sigma_l/\sigma_e)^2} + \delta\tau_m . \end{aligned} \tag{13}$$

The stationary condition allows one to express the width of the detuning curve $\delta\tau_m$ in the form

$$\delta\tau_m = P\tau_0 \frac{\sigma_l^2}{\sigma_l^2+\sigma_e^2}. \tag{14}$$

Making use of Eq. (11), one can solve for τ_0 the previous relation and express $\delta\tau_m$ as a function of the peak gain g_0, the cavity losses P, and the rms widths of the laser pulse (σ_l) and of the electron bunch (σ_e):

$$\delta\tau_m = P \frac{\sigma_l^2}{\sqrt{\sigma_e^2+\sigma_l^2}} \sqrt{2 \ln\left[\frac{(1-P)g_0}{P\sqrt{1+(\sigma_l/\sigma_e)^2}} \right]}. \tag{15}$$

While the use of Eq. (14) requires (at least) the preliminary measurements of τ_0 (which is a parameter difficult to be predicted), Eq. (15) may be, in principle, employed for estimating $\delta\tau_m$ before any measurements. For this, σ_l can be, in the first approximation, expressed in terms of σ_e according to the relation [6] $\sigma_l \simeq \sqrt{\Delta\sigma_e}$ [where $\Delta = (N+N_d)\lambda_r$ is the so-called slippage factor], σ_e is, by hypothesis, constant, g_0 may be calculated by means of Eq. (3), and P is normally theoretically known from the mirror design.

C. Conservation of the second-order moment

The conservation of the second-order moment

$$\int_{-\infty}^{+\infty} (\tau-\tau_f)^2 I_f(\tau)\, d\tau = \int_{-\infty}^{+\infty} (\tau-\tau_0)^2 I(\tau)\, d\tau \tag{16}$$

coincides with that of the rms value of the laser distribution: $\sigma_{lf}^2 = \sigma_l^2$ (where σ_{lf} is the rms value of the distribution I_f). Making use of Eqs. (8) and (11), one gets

$$\begin{aligned}\sigma_{lf}^2 &\equiv \frac{\int_{-\infty}^{+\infty} (\tau-\tau_f)^2 I_f(\tau)\, d\tau}{\int_{-\infty}^{+\infty} I_f(\tau)\, d\tau} \\ &= \sigma_l^2 \frac{1+R^2(\sigma_l/\sigma_e)^2}{1+(\sigma_l/\sigma_e)^2} + R^2 \left(\frac{\tau_0^2(\sigma_l/\sigma_e)^2}{1+(\sigma_l/\sigma_e)^2} \right)(1-R^2), \end{aligned} \tag{17}$$

which, combined with condition (16), gives

$$\left(\frac{\sigma_l}{\sigma_e}\right)^2 = \left(\frac{R\tau_0}{\sigma_e}\right)^2 - 1. \tag{18}$$

This relation connects the rms value σ_l of a fully detuned laser to the position τ_0 of its centroid and can be fulfilled only if

$$\frac{\tau_0}{\sigma_e} > 1/R \simeq 1. \tag{19}$$

The previous condition shows that the rms value σ_l may be not conserved. This leads to the conclusion that the temporal distribution of a saturated SRFEL is not necessarily stationary or, at least, not necessarily Gaussian. The important question arising from this result, namely, the general conditions under which a saturated SRFEL reaches a completely stationary regime, is beyond the scope of this paper and would deserve a dedicated analysis.

If the condition (19) is satisfied, the relation (18) can be used to get rid of the dependence on σ_l in the expressions for the peak gain [Eq. (11)] and for the width of the detuning curve [Eq. (14)]. In the first case, one finds

$$g_O = \frac{P}{\sqrt{(1-P)}} \exp\left[\frac{1}{2(1-P)} \right] \frac{\tau_0}{\sigma_e}, \tag{20}$$

while in the second case one obtains

$$\delta\tau_m = \frac{P}{1-P} \frac{1}{\tau_0} [(1-P)\tau_0^2 - \sigma_e^2]. \tag{21}$$

It is worthwhile to stress that, while the formulas (11) and (20) supply an agile ''on-line'' method (alternative to those mentioned in Sec. II) for the measurement of the laser-off peak gain, relations (14) and (21) yield a significant insight into the physics of the laser–electron-beam interaction.

IV. COMPARISON WITH EXPERIMENTS

The theoretical model presented in the preceding section is based on the assumptions that when the laser reaches the saturation regime, the electron beam is characterized by a stable temporal distribution having a Gaussian profile. In re-

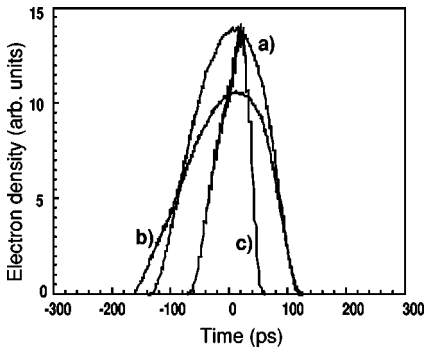

FIG. 4. Effect of the harmonic cavity on the shape and on the rms value of the Super-ACO electron beam (the beam current is about 40 mA). Curve *a*: passive harmonic cavity. Curve *b*: harmonic cavity powered at 80 kV. Curve *c*: harmonic cavity powered at 300 kV.

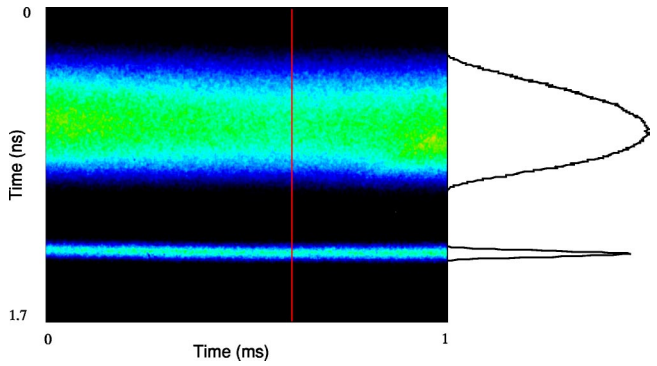

FIG. 5. (Color online) Streak camera image of the Super-ACO electron bunch (upper trace) and laser macropulse (lower trace). A vertical cut provides the beam (laser) temporal distribution. The total vertical scale is 1.7 ns and the longitudinal scale is 1 ms The image has been taken for a total beam current of 55 mA with the harmonic cavity set in the passive configuration.

ality, the electron-beam dynamics is generally influenced by the beam interaction with the ring environment (e.g., the metallic wall of the vacuum chamber). Such interaction manifests itself as a ''wake'' electromagnetic field that acts on the electrons and may perturb their stability. The so-called microwave instability [21] is one of the most likely observed: it leads to an increase of the beam energy spread, which may induce a low-frequency (about 100 Hz) oscillation of the bunch length [25,26]. High-frequency (tens of kilohertz) instabilities are also observed: they normally lead to a coherent oscillation of the electron beam at the synchrotron frequency and (eventually) its harmonics [25].

The interplay between electron-beam instabilities and the FEL dynamics has been the subject of various investigations [22,23,27]. It is nowadays a common opinion that the instability and the laser growth may be considered as competitive phenomena: either the instability is strong enough to prevent the laser onset or the laser is able to develop and damp (or, at least, reduce) the instability effect. As a consequence, the temporal distribution of the electron beam can be actually considered as (almost) stable when the laser has reached the steady state.

The other assumption, i.e., the Gaussian shape of the beam profile, is more delicate. In fact, the interaction with the ring environment induces also a perturbation of the ''natural'' Gaussian profile of the electron beam. In the case of Super ACO, due to the relative high value of the ring impedance [28], this effect is quite noticeable. Furthermore, the distortion becomes more evident when a harmonic cavity is used [29,34], which has been installed in order to shorten the bunch length and increase the amplification gain. Figure 4 shows the temporal profile of the electron beam for different settings of the harmonic cavity. The distortion of the electron-beam profile with respect to the ideal Gaussian shape represents the main limitation to the method derived in Sec. III. However, as it will be clear in the following, relations (11) and (14) [as well as Eqs. (20) and (21)] still remain reliable, also when the harmonic cavity is active (and powered at 80 kV; see Fig. 4, profile b). It is, moreover, worthwhile to point out that the distortion of the beam profile due to the ''wake'' field is expected to play a minor role for the case of third generation SRFELs, such as ELETTRA, which are generally characterized by smoother ring vacuum chambers [28]. The other relevant hypothesis on the electron beam which has been employed for deriving Eq. (8), i.e., σ_e constant during the onset of the fully detuned laser pulse, has been validated during a series of experiments that have been performed on the Super-ACO FEL.

In order to apply the formulas that have been derived in Sec. III and check the validity of the theoretical model on which they are based, the statistical parameters of the coupled laser and electron-beam distributions have been measured for different experimental settings. In this purpose, a double-sweep streak camera has been used [30–32]. Figure 5 shows the kind of image that can be obtained by acquiring at the same time the synchrotron light emitted by a bending magnet (which reproduces the temporal structure of the electron bunches) and the laser signal. The (coupled) temporal profiles of the electron bunch and laser distributions can be found by taking a vertical cut of the whole picture. Along the horizontal direction, one can follow the temporal evolution of the two distributions. Collecting a series of pictures for different detuning amounts allows one to measure the variation of the position occupied by the laser centroid with respect to the position corresponding to the perfect synchronism.

The losses of the optical cavity have been measured *in situ* by determining the decay time of the light intensity when the detuning is strong enough to prevent the laser onset [33]. Figure 6 shows the laser-off peak gain (as a function of the beam current) as it is obtained using Eq. (11). Two cases are presented: one in which the harmonic cavity is passive and one in which the harmonic cavity is powered at 80 kV. In both cases the results are found to be in a fairly good agreement with the estimations supplied, e.g., by Eq. (3) [35] or by the measurement of the initial growth rate of the laser intensity [36]. The gain calculated by using the maximum detuning method is also in agreement with the direct measurement corresponding to the beam current threshold for the laser oscillation.

In Figs. 7 and 8 the direct measurement of the width of

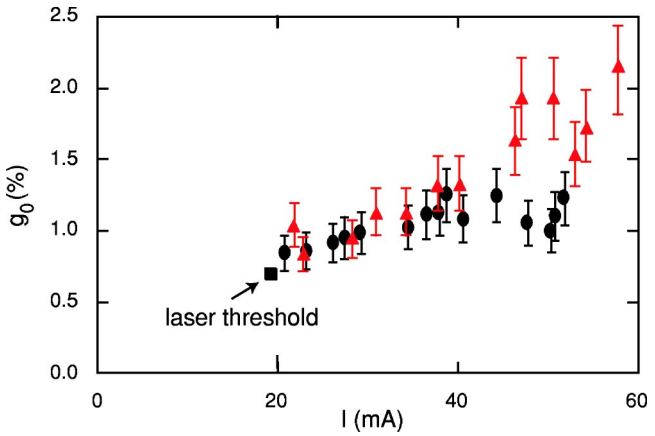

FIG. 6. (Color online) Behavior of the laser-off peak gain g_0 of the Super-ACO FEL as a function of the total beam current I, as it is obtained using Eq. (11); full circles refer to the configuration in which the harmonic cavity is passive while filled triangles refer to the case in which the harmonic cavity is powered at 80 kV. The relative error (around 15%) is mainly due to the uncertainty on the measurement of the cavity losses. The square represents the gain (directly measured) corresponding to the beam current threshold for the laser oscillation (for the configuration in which the harmonic cavity is passive).

the detuning curve (see Fig. 1) is compared with the result obtained by using the maximum detuning method [i.e., Eq. (14)]. Here again, in the first case the harmonic cavity is passive and in the second case it is powered at 80 kV. The results show in both cases a good agreement and allow for a straight experimental validation of the theoretical approach proposed in this paper.

It is finally worthwhile to mention that the condition (19) is not always (i.e., for any beam current and cavity mirror setting) fulfilled. As a consequence, the relations (20) and (21) are not always employable. However, when the condition (19) is respected, they lead to a result in agreement with that supplied, respectively, by relations (11) and (14).

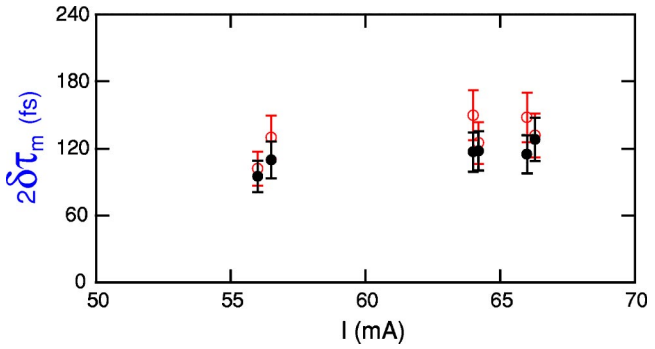

FIG. 7. (Color online) Behavior of the full width of the detuning curve $2\delta\tau_m$ as a function of the total beam current I, as it is obtained by directly measuring the maximum detuning compatible with the laser onset (full circles) and as it is obtained by means of the maximum detuning method (empty circles), see Eq. (14). The harmonic cavity is set in the passive configuration.

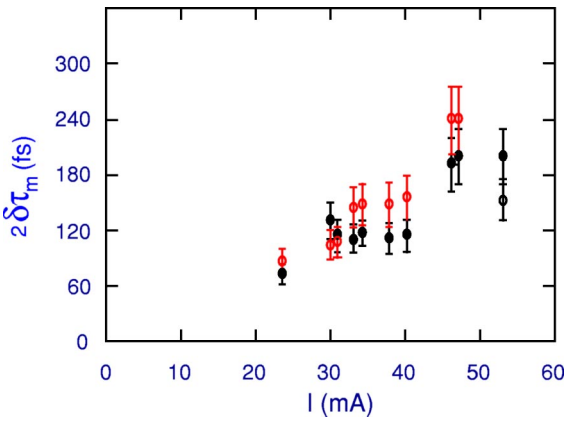

FIG. 8. (Color online) The same as Fig. 7 with the harmonic cavity powered at 80 kV.

V. CONCLUSIONS

The analysis carried out in this paper provides a theoretical picture of the steady state of a fully detuned SRFEL. In particular, an ''agile'' method for the evaluation of the laser-off peak gain has been derived, which is an alternative to those relying on Madey's theorem and on the evaluation of the initial growth rate of the laser intensity. Moreover, a step further has been made in the understanding of the interplay between the maximum laser–electron-beam detuning (compatible with the laser onset) and the physical parameters leading the dynamics of a SRFEL. The equilibrium distribution of a fully detuned SRFEL has been shown to be not necessarily Gaussian. This entails that the result obtained for the case of a quasizero laser–electron-beam detuning by means of the method of the ''supermodes,'' cannot be simply extended to the case of a fully detuned system. This result arises the question about the actual existence of a completely stationary regime of a detuned SRFEL. Theoretical results have been compared with measurements performed on the Super-ACO FEL. The obtained agreement can be considered as satisfactory.

ACKNOWLEDGMENTS

We are particularly thankful to M. Billardon for having driven our attention to the subject treated in this paper and to G. Dattoli and D. Fanelli for enlightening discussions. The support by the TMR Network, Grant No. ERB4061PL97-0102, is acknowledged.

APPENDIX

In this appendix some details of the calculations reported in Sec. III are given relative to the conservation of the first moments of the stationary fully detuned laser distribution.

Zero-order moment

The zero-order moment of the temporal profile of the laser pulse $I_n(\tau)$ (i.e., the laser intensity after the nth interaction) is defined by

$$M_{0,n}=\int_{-\infty}^{+\infty} I_n(\tau)d\tau. \tag{A1}$$

Assuming that the laser has reached the steady state in the condition of maximum detuning and that the equilibrium distribution is Gaussian [see Eq. (7)], the zero-order moment reads

$$M_0=I_0\int_{-\infty}^{+\infty}\exp[-(\tau-\tau_0)^2/2\sigma_l^2]d\tau=I_0\sqrt{2\pi}\sigma_l. \tag{A2}$$

The zero-order moment of the steady-state distribution can be also calculated starting from Eq. (8) [37]:

$$\begin{aligned}M_0&=\int_{-\infty}^{+\infty} I_f(\tau)d\tau\\&=R^2I_0\int_{-\infty}^{+\infty}\exp[-(\tau-\tau_0-\delta\tau_m)^2/2\sigma_l^2]\\&\quad\times\left\{1+g_0\exp\left[-\frac{(\tau-\delta\tau_m)^2}{2\sigma_e^2}\right]\right\}d\tau\\&=R^2I_0\sqrt{2\pi}\sigma_l+R^2I_0g_0\sqrt{2\pi}\sigma_l\frac{\exp\{-\tau_0^2/[2(\sigma_e^2+\sigma_l^2)]\}}{\sqrt{1+(\sigma_l/\sigma_e)^2}}.\end{aligned} \tag{A3}$$

The combination of Eqs. (A2) and (A3) leads to Eq. (10) and then to the relation (11) expressing the laser-off peak gain as a function of the cavity losses and the statistical parameters of the laser and electron-beam distributions.

First-order moment

The first-order moment of the laser pulse

$$M_{1,n}=\int_{-\infty}^{+\infty}\tau I_n(\tau)d\tau \tag{A4}$$

coincides (if normalized to $M_{0,n}$) with the position of the laser centroid:

$$\tau_n\equiv\frac{M_{1,n}}{M_{0,n}}. \tag{A5}$$

In the case of a fully detuned steady state, the laser pulse (assumed to be Gaussian) may be expressed as in Eq. (7) and is, therefore, assumed to be centered around τ_0:

$$\tau_0=\frac{M_0}{M_1}=\frac{1}{\sqrt{2\pi}\sigma_l}\int_{-\infty}^{+\infty}\exp[-(\tau-\tau_0)^2/2\sigma_l^2]d\tau. \tag{A6}$$

The first-order moment of the steady-state distribution can be also calculated starting from Eq. (8) [37]:

$$M_0=\int_{-\infty}^{+\infty}\tau I_f(\tau)d\tau=R^2I_0(\tau_0+\delta\tau_m)\sqrt{2\pi}\sigma_l+R^2I_0g_0\sqrt{2\pi}\frac{[\tau_0\sigma_e^2+\delta\tau_m(\sigma_e^2+\sigma_l^2)]\sigma_e\sigma_l\exp\{-\tau_0^2/[2(\sigma_e^2+\sigma_l^2)]\}}{(\sigma_e^2+\sigma_l^2)^{3/2}}. \tag{A7}$$

The definition of τ_f,

$$\tau_f\equiv\frac{\int_{-\infty}^{+\infty}\tau I_f(\tau)d\tau}{\int_{-\infty}^{+\infty} I_f(\tau)d\tau}, \tag{A8}$$

leads [recalling Eq. (A3)] to Eq. (13) and thus, imposing the stationary condition $\tau_f=\tau_0$, to the expression (14) for the maximum detuning (i.e., the half-width of the detuning curve).

Second-order moment

The second-order moment of the laser pulse

$$M_{2,n}=\int_{-\infty}^{+\infty}(\tau-\tau_n)^2 I_n(\tau)d\tau \tag{A9}$$

gives (if normalized to $M_{0,n}$) the rms value of the laser distribution:

$$\sigma_n^2=\frac{M_{2,n}}{M_{0,n}}. \tag{A10}$$

In the case of a fully detuned steady state, the laser pulse (assumed to be Gaussian) may be expressed as in Eq. (7) and is, therefore, assumed to have a given rms value σ_l. The expression of σ_{lf} can be calculated [37] as in Eq. (17). The stationary condition $\sigma_l=\sigma_{lf}$ leads to Eq. (18) and thus to the condition (19).

[1] M.E. Couprie *et al.*, Nucl. Instrum. Methods Phys. Res. A **331**, 37 (1993).
[2] H. Hama *et al.*, Nucl. Instrum. Methods Phys. Res. A **375**, 32 (1996).
[3] M. Trovò *et al.*, Nucl. Instrum. Methods Phys. Res. A **483**, 157 (2002).
[4] M. Billardon *et al.*, Phys. Rev. Lett. **69**, 2368 (1992).
[5] A. Renieri, Riv. Nuovo Cimento **53B**, 161 (1979).
[6] G. Dattoli *et al.*, Phys. Rev. A **37**, 4326 (1988).
[7] G. Dattoli *et al.*, Phys. Rev. A **37**, 4334 (1988).
[8] V.N. Litvinenko *et al.*, Nucl. Instrum. Methods Phys. Res. A **358**, 369 (1995).
[9] V.N. Litvinenko *et al.*, Nucl. Instrum. Methods Phys. Res. A **358**, 334 (1995).
[10] G. Dattoli *et al.*, Phys. Rev. E **55**, 2056 (1997).
[11] G. De Ninno *et al.*, Phys. Rev. E **65**, 056504 (2002).
[12] G. De Ninno, Nucl. Instrum. Methods Phys. Res. A **483**, 152 (2002).
[13] V.N. Litvinenko, Nucl. Instrum. Methods Phys. Res. A **475**, 240 (2001).
[14] G. De Ninno *et al.*, Phys. Rev. E **64**, 026502 (2001).
[15] M.E. Couprie *et al.*, Nucl. Instrum. Methods Phys. Res. A **358**, 374 (1995).
[16] S. Koda *et al.*, Nucl. Instrum. Methods Phys. Res. A **475**, 211 (2001).
[17] P. Elleaume, J. Phys. (Paris) **45**, 997 (1984).
[18] J.M.J. Madey, J. Appl. Phys. **42**, 1906 (1971).
[19] N.A. Vinokurov *et al.*, Report No. INP77.59, 1977 (unpublished).
[20] W. Colson and P. Elleaume, Appl. Phys. B: Photophys. Laser Chem. **29**, 101 (1982).
[21] G. Dattoli and A. Renieri, Nucl. Instrum. Methods Phys. Res. A **375**, 1 (1996).
[22] M. Migliorati and L. Palumbo, Nuovo Cimento Soc. Ital. Fis., A **112**, 461 (1999).
[23] H. Hama *et al.*, Nucl. Instrum. Methods Phys. Res. A **341**, 12 (1994).
[24] M. Billardon, Super-ACO internal note (unpublished).
[25] R. Roux, Ph.D. thesis, Université Paris 6, 1999 (unpublished).
[26] R. Roux and M. Billardon, Nuovo Cimento Soc. Ital. Fis., A **112A**, 513 (1999).
[27] R. Bartolini *et al.*, Phys. Rev. Lett. **87**, 134801 (2001).
[28] G. Dattoli *et al.*, Nucl. Instrum. Methods Phys. Res. A **471**, 403 (2001).
[29] M. Billardon *et al.*, Proceedings of EPAC 1998 (unpublished) http://accelconf.web.cern.ch
[30] R. Roux *et al.*, Nucl. Instrum. Methods Phys. Res. A **393**, 33 (1997).
[31] H. Hama *et al.*, Nucl. Instrum. Methods Phys. Res. A **358**, 365 (1995).
[32] A.H. Lumpkin *et al.*, Nucl. Instrum. Methods Phys. Res. A **393**, 50 (1997).
[33] D. Nutarelli, Ph.D. thesis, Université Paris 6, 2000 (unpublished).
[34] R.P. Walker *et al.*, Nucl. Instrum. Methods Phys. Res. A **429**, 179 (1999).
[35] C. Bruni, DEA Report 2001 (unpublished).
[36] D. Garzella *et al.*, Proceedings of EPAC 2002 (unpublished), http://accelconf.web.cern.ch
[37] I.S. Gradshteyn and I.M. Ryzhik, *Table of Integrals, Series and Products* (Academic Press, London, 1980).